The Journal of Experimental Biology 214, 3727-3731

doi:10.1242/jeb.057323

METHODS & TECHNIQUES

Non-invasive study of *Octopus vulgaris* arm morphology using ultrasound

Laura Margheri[1,*], Giovanna Ponte[2,*], Barbara Mazzolai[3], Cecilia Laschi[1] and Graziano Fiorito[2,†]

[1]The BioRobotics Institute, Scuola Superiore Sant'Anna, 56025, Pontedera, Pisa, Italy, [2]Stazione Zoologica Anton Dohrn, Villa Comunale, 80121 Napoli, Italy and [3]Center for MicroBioRobotics@SSSA, Istituto Italiano di Tecnologia (IIT), 56025 Pontedera, Pisa, Italy

*These authors contributed equally to this work
†Author for correspondence (graziano.fiorito@szn.it)

Accepted 22 August 2011

SUMMARY

Octopus arms are extremely dexterous structures. The special arrangements of the muscle fibers and nerve cord allow a rich variety of complex and fine movements under neural control. Historically, the arm structure has been investigated using traditional comparative morphological *ex vivo* analysis. Here, we employed ultrasound imaging, for the first time, to explore *in vivo* the arms of the cephalopod mollusc *Octopus vulgaris*. Sonographic examination (linear transducer, 18 MHz) was carried out in anesthetized animals along the three anatomical planes: transverse, sagittal and horizontal. Images of the arm were comparable to the corresponding histological sections. We were able, in a non-invasive way, to measure the dimensions of the arm and its internal structures such as muscle bundles and neural components. In addition, we evaluated echo intensity signals as an expression of the difference in the muscular organization of the tissues examined (i.e. transverse *versus* longitudinal muscles), finding different reflectivity based on different arrangements of fibers and their intimate relationship with other tissues. In contrast to classical preparative procedures, ultrasound imaging can provide rapid, destruction-free access to morphological data from numerous specimens, thus extending the range of techniques available for comparative studies of invertebrate morphology.

Supplementary material available online at http://jeb.biologists.org/cgi/content/full/214/22/3727/DC1

Key words: arm, echo intensity, morphology, octopus, ultrasound.

INTRODUCTION

Cuttlefish, squid and octopus show striking modifications of the molluscan bauplan (Packard, 1972; Runnegar and Pojeta, 1974; House, 1988): the shell is greatly reduced or lost, the mantle is co-opted for new functions, and the ventral foot is modified into prehensile arms. The extremely flexible arms, arranged around the mouth to form a brachial crown, are of particular advantage for predators like cephalopods. They are effectively used to obtain and manipulate prey during feeding (Packard, 1972; Wells, 1978; Hanlon and Messenger, 1996; Grasso, 2008).

Animals use their arms to perform a rich variety of complex movements with high performance and sophisticated neural control (Chichery and Chichery, 1988; Gutfreund et al., 1996; Sumbre et al., 2001; Huffard et al., 2005; Sumbre et al., 2005; Finn et al., 2009). The complexity of maneuvers, and postural and locomotor capabilities of the cephalopods' eight arms reach their pinnacle in octopuses. In these species each one of the eight arms can elongate, shorten, twist, bend and exert considerable force (Dilly et al., 1964). The extreme variety of movements achieved in the octopus largely contributes to the complexity of its behavioral repertoire (Mather 1998; Borrelli et al., 2006).

The complexity of these maneuvers, in the absence of any hard skeletal elements, represents a source of inspiration for engineers and roboticists with the aim of designing a new class of highly dexterous bioinspired robots (Walker et al., 2005; Laschi et al., 2009).

Cephalopod arms function in the absence of any hard skeletal structure, and are defined as muscular hydrostats (Kier, 1982; Kier and Smith, 1985). Arms of all coleoids show a similar design; they are essentially composed of a three-dimensional arrangement of muscle fibers surrounding a central axis occupied by a nerve cord (Kier and Smith, 1985; Kier, 1985).

A relevant body of knowledge is available on the morphology of the octopus arm (Cuvier, 1817; Colasanti, 1876; Guérin, 1908; Graziadei, 1971; Kier and Stella, 2007). Briefly, each arm is composed of a series of fibers assembled along three dimensions: perpendicular to the long axis (transverse muscle), parallel to the long axis (longitudinal muscle), and helical or oblique around the long axis (helical or oblique muscles). The complexity of the structure of an octopus arm has been deduced through a series of studies applying different morphological approaches.

Here, we employed ultrasound imaging for the first time to explore *in vivo* the arms of *Octopus vulgaris*. Our aim was to identify internal parts of the arms in living animals as they appear in the classic morphological post mortem studies, thus discriminating the different assemblage of muscular structures *in vivo*. The final goal was to promote a new experimental approach by using the ultrasound technique, which may assist in reaching internal targets and, consequently, reducing the impact of surgery and also improving accuracy. In addition, this approach may reveal changes in muscle thickness during contraction and relaxation of different fibers.

MATERIALS AND METHODS

Animals

A total of 12 *O. vulgaris*, Cuvier 1797, of both sexes (body mass range, 250–730 g), fished in the Bay of Napoli (Italy), were used

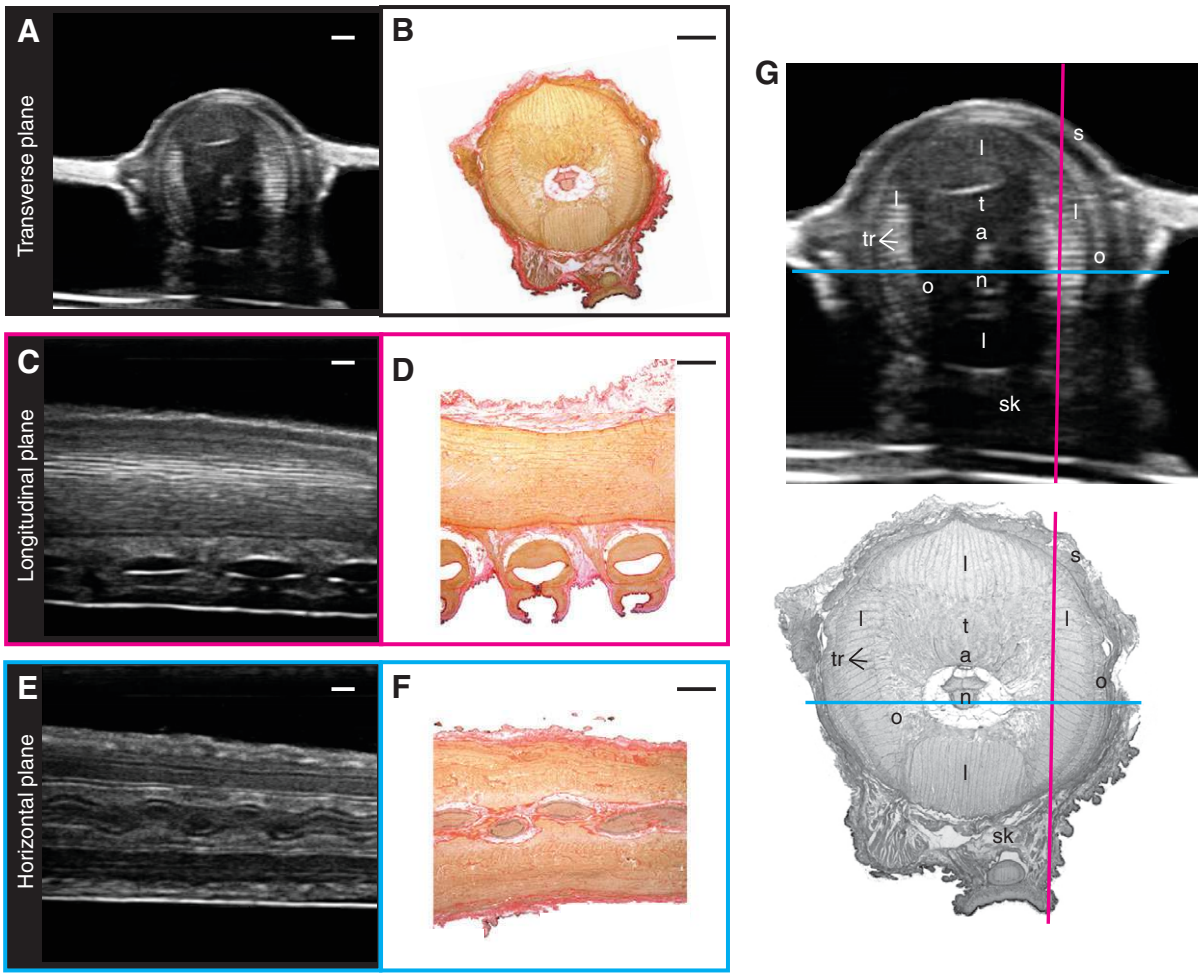

Fig. 1. The arm of *Octopus vulgaris* as it appears in sonographic scans (A,C,E) and corresponding histological sections (Picro Ponceau stain; B,D,F). Scale bar, 2.0 mm. The same sonographic scan and histological section of the transverse plane (A,B) are annotated in G: s, skin; l, longitudinal muscle fibers; t, transverse muscle fibers; a, artery; n, nerve cord; tr, trabeculae; o, oblique muscle layer; sk, sucker. The two lines, in magenta and cyan, indicate the level of sections in the horizontal and sagittal planes, respectively. See text for details.

in this study. Animals were maintained in tanks under conditions similar to those described by Fiorito et al. (Fiorito et al., 1990). Octopuses were fed a live crab (*Carcinus mediterraneus*) every other day.

Anesthesia

Animals were anesthetized by immersion in an anesthetic solution (3.5% $MgCl_2$ in sea water) (see Messenger et al., 1985). Five minutes of anesthesia were sufficient to minimize the spontaneous movements of the animal; 10 min were required for the animal to be completely relaxed; 15 min in the anesthetic solution completely stopped the octopus breathing, while 30 min were necessary to reach deep anesthesia (Grimaldi et al., 2007). Ultrasound examination was carried out in completely relaxed octopuses (i.e. 10 min anesthesia).

Sonographic approaches

We used an Esaote MyLab^{TM}Five VET ultrasound imager (Genoa, Italy) with an LA435 transducer (18 MHz). The axial and lateral resolution limits of the equipment were 0.085 and 0.104 mm, respectively. Ultrasound examination was carried out in a small circular chamber filled with 31 of anesthetic solution into which each octopus was transferred. Measurements were made using a device described elsewhere (Grimaldi et al., 2007). In brief, the device had a circular base (diameter, 39 cm), which was placed on the examination tank, and a central rectangular opening into which a holder (where the transducer was fixed) could be placed and moved horizontally (movement range, 13 cm) to allow scanning of animal. All sonographic images were stored for further analysis.

Examination of the arms and measurement of the dimensions of different parts was done in real time (2D mode) using images in which the profile of the arms was completely and clearly outlined (Goldstein et al., 1987; Zagzebski, 1996). All system-setting parameters, such as gain (79%), dynamic range (11), sharpness (3) and depth (3 cm) were kept constant throughout the sonographic examination. In addition, we fixed the exact site of any measurement at a given anatomically defined location, for each arm, in order to ensure replicability in different individuals and to identify samples to be processed for histology. Timing was standardized in order to allow examination of the arms in the same relaxed conditions.

Three sonographic scanning planes were utilized on the basis of the proximo-distal axis of the arm: transverse, horizontal and longitudinal. In the transverse plane the probe was perpendicular to the longitudinal axis of the arm, and moved from the proximal to

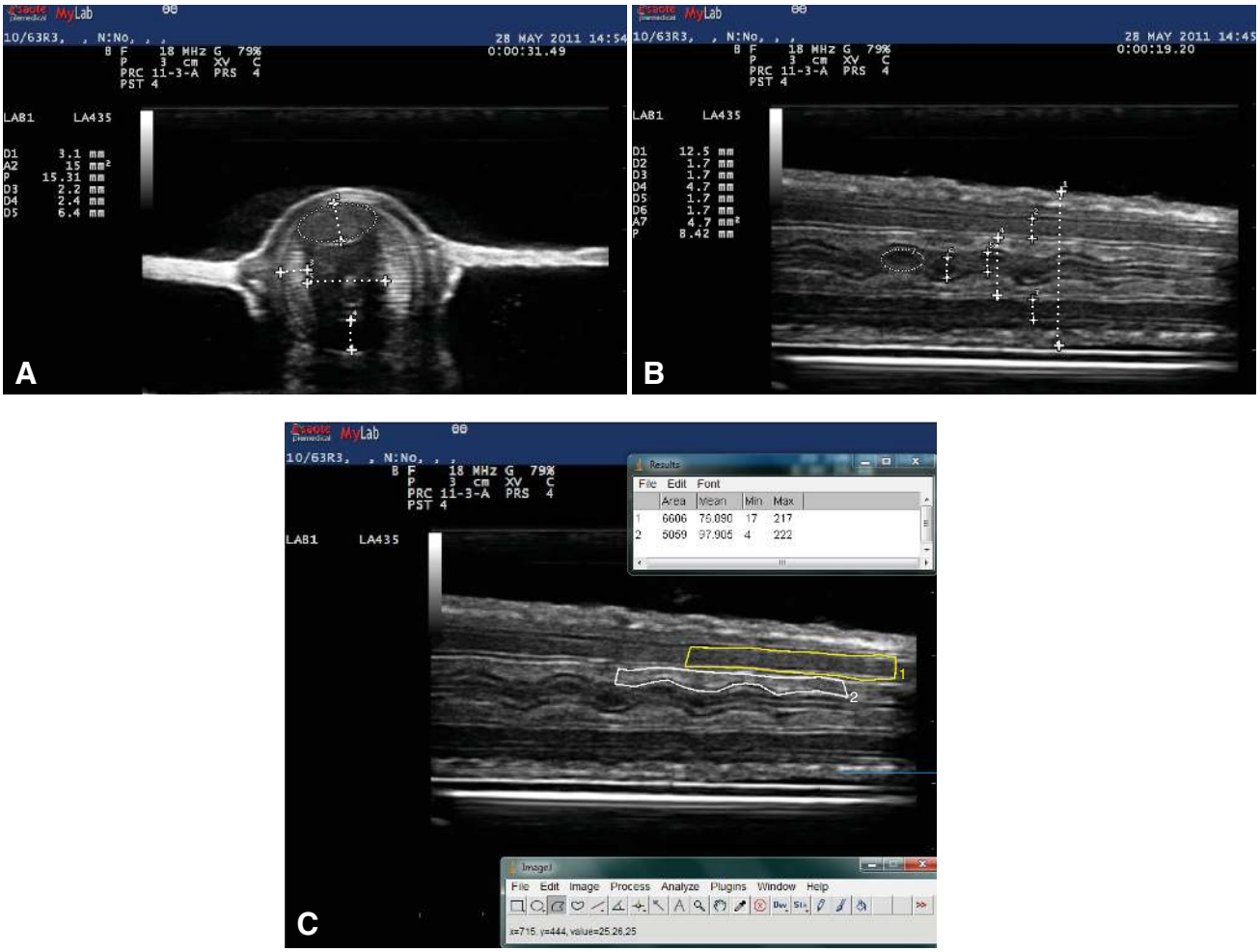

Fig. 2. Snapshots from the sonographic examination of the octopus arm to evaluate the dimensions of internal structures (A,B) and echo intensities of different muscle bundles (C) *in vivo*. (A) Transverse plane, dorsal longitudinal fibers (D1, mm) and corresponding area (A2, mm^2), lateral and ventral longitudinal fibers (D3 and D4, respectively), and latero-lateral extensions of transverse fibers (D5). (B) Horizontal plane, latero-lateral extension of the entire arm (D1), lateral longitudinal fibers (D2, D3), latero-lateral extensions of transverse fibers (D4), nerve cord (D5, D6) and area of a ganglion (A7, mm^2). Measurements were taken at the same level of scanning. (C) Example of a gray-scale analysis of the longitudinal (yellow, 1) and transverse (white, 2) muscles. Regions of interest are drawn within the borders of the muscle. The results of mean muscle echo intensity together with area and minimum and maximum values for each region are shown using ImageJ analysis tool.

the distal end. Sagittal sections were obtained with the probe parallel to the longitudinal axis (latero-lateral extension). Finally, the horizontal scanning started from the ventral side (suckers) by moving the probe towards the dorsal side of the arm.

The digital calipers were positioned on the outline of each identifiable muscle bundle. The reproducibility of ultrasonographic measurements was assessed over 2 consecutive days by measuring the extension of the transverse fibers (transverse plane) and nerve cord (sagittal and horizontal planes), keeping the anatomical location of a given arm of the same individual constant (see Grimaldi et al., 2007).

In a few instances, ultrasound examination was carried out on live, unrestrained animals to visualize the arm in its dynamic state.

Internal morphology

Animals (N=3) were deeply anesthetized as described above and a proximal part of the right anterior arm (R1; about 50 mm length) was dissected. Samples were immediately fixed overnight in 4% paraformaldehyde (in 0.1 mol l^{-1} phosphate buffer, pH 7.6, osmolarity controlled). They were then dehydrated in ethanol and embedded in paraffin. Blocks were sectioned by a rotary microtome (Leica RM2245); serial sections (10 μm) were obtained in the three planes, collected on chrome–alum–gelatin-coated slides, and stained with Picro Ponceau (see Kier, 1992).

Measurement of echo intensity

The mean echo intensity was determined following the method of Scholten and colleagues (Scholten et al., 2003) (see also Pillen et al., 2009) in selected areas of interest, using ImageJ (Abramoff et al., 2004). Independent-sample t-test was applied to mean intensity values in order to evaluate whether muscle fibers arranged in different bundles show significant differences in their relative echo intensity.

Statistical analysis was done using the SPSS package for Windows 18 (SPSS Inc., Chicago, IL, USA).

RESULTS

In Fig. 1, typical sonographic images of the octopus arm are shown and compared with histological sections corresponding to the same anatomical plane.

Table 1. Mean and standard errors (range in parentheses) of dimensions of various structures identified in an *Octopus vulgaris* arm

	Ultrasound		Histology		*r*	*P*
Transverse plane						
Dorsal longitudinal thickness	3.09±0.07	(2.8–3.4)	2.76±0.04	(2.6–3.0)	0.72	0.018
Cross-sectional area	15.31±0.29	(13.4–16.2)	11.02±0.18	(10.2–11.9)	0.69	0.025
Lateral longitudinal thickness	2.19±0.04	(2.0–2.4)	1.64±0.03	(1.5–1.8)	0.81	0.005
Ventral longitudinal thickness	2.37±0.06	(2.1–2.7)	2.20±0.06	(2.0–2.5)	0.76	0.009
Transverse thickness	6.37±0.07	(6.0–6.7)	5.44±0.12	(5.0 –6.1)	0.69	0.025
Horizontal plane						
Transverse thickness	4.73±0.08	(4.3–5.1)	3.97±0.08	(3.7–4.2)	0.79	0.006
Nerve cord ganglion extension	1.67±0.05	(1.4–1.9)	1.16±0.03	(1.0–1.3)	0.74	0.007
Cross-sectional area	4.57±0.09	(4.3–5.0)	4.16±0.07	(3.9–4.7)	0.80	0.005

For muscle bundles: thickness and cross-sectional area; for a ganglion in the nerve cord: longitudinal extension and area. Measurements were taken at the same anatomical position and from the same arms of two animals (N=10). All extensions are given in mm, areas in mm^2. Results of Pearson's correlations (r) between measurements taken during sonographic examination and comparable histological sections of arm taken post mortem are also given.

In the transverse plane we could see the entire arm (Fig. 1A,B). Its external outline is clearly visible with the skin and its folds (see Fig. 1G, s) appearing bright. Medially, two bundles of longitudinal muscle fibers are visible (dorsal and ventral; see Fig. 1G, l); they appear darker than other structures. Below the dorsal longitudinal fibers, an H-shaped structure (transverse fibers; see Fig. 1G, t) of similar echo intensity appears, well defined by bright borders. On both sides of the 'H', and to complete the circular shape of the arm in this plane, another set of longitudinal muscles is revealed (see Fig. 1G, l).

Longitudinal fibers are mixed with laminae of fibrous connective tissue, i.e. trabeculae (Fig. 1) (see also Kier and Stella, 2007). In the lateral longitudinal bundles, the trabeculae appear as parallel reflecting sheets which provide higher values of echo intensity when compared with the dorsal and ventral longitudinal bundles. Indeed, in the dorsal and ventral areas, trabeculae are arranged along the dorso-ventral axis of the arm and their reflectance is not detected by the probe. This results in different values of echo intensity. Finally, external oblique muscles are visible (see Fig. 1G, o). In addition, median and internal oblique muscles are recognized during scanning by their lower echo intensity relative to surrounding structures. In the center of the arm two structures with higher echo intensity are revealed: the artery (see Fig. 1G, a) and nerve cord (see Fig. 1G, n), dorsal and ventral, respectively. Sonographic scanning also detects the two axon tracts within the nerve cord, below the artery. Finally, above each sucker (see Fig. 1G, sk) a bright line is visible corresponding to the brachial ganglion.

In this plane, as the scanning proceeds along the arm, the sinusoidal arrangement of the nerve cord appears as a result of the relative position of the brachial ganglia of two paired suckers.

In the longitudinal plane, the sonographic examination reveals the same structures as described above, from the skin to the external oblique and longitudinal fibers (Fig. 1C,D). As the scan proceeds, the transverse muscles are identified and became distinguishable from the longitudinal ones by their different reflectivity (image not shown). When approaching the centre of the arm, the artery and the nerve cord are clearly visible; in addition, the serial arrangement of the brachial ganglia becomes evident, corresponding to the suckers of the same side. This confirms the sinusoidal arrangement of the nerve cord along the arm (Graziadei, 1971). Finally, on the ventral side the longitudinal muscles appear quite distinct from the intrinsic musculature of the sucker.

In the horizontal plane, as the scanning proceeds along the arm (dorsal to ventral), structures with different echo intensity are revealed and easily compared with histological sections (data not shown). Among the different scans, the image where the internal structures of the arm are easily identifiable is the medial one (Fig. 1E,F). In this picture, from side to side, external, medial and internal oblique muscles are clearly distinguished by their reflectivity in respect to other structures. Longitudinal and transverse fibers are also revealed. It is in this plane that the sinusoidal arrangement of the nerve cord is maximally evident.

Following Grimaldi et al. (Grimaldi et al., 2007), sonographic measurements of muscle bundles and ganglia of the nerve cord were correlated with those determined post mortem in histological sections (Fig. 2). Significant Pearson's correlations were obtained for measurements of muscle thickness, muscle cross-sectional area and extension, and area of a ganglion in the nerve cord (Table 1).

In addition, values of muscle echo intensity measured in the three scanning planes were also determined (Table 2). In our conditions, longitudinal and transverse muscle fibers appear significantly different (P<0.001, after t-test; see Table 2) in all three planes and also when longitudinal lateral (including trabeculae, in transverse and horizontal planes) or dorsal longitudinal (sagittal plane) fibers are considered.

Ultrasonographic scans were also achieved on the arms of freely moving, un-anesthetized octopuses, revealing the structures during dynamic action (see supplementary material Movies 1 and 2).

Table 2. Mean and standard errors of echo intensity measurements of transverse and longitudinal fibers of *Octopus vulgaris* arm

	N	Transverse	Longitudinal	*t*	d.f.	*P*
Transverse plane	48	29.3±1.5	90.9±2.9	18.4	94	<0.001
Sagittal plane	24	26.3±2.1	55.7±3.9	6.5	46	<0.001
Horizontal plane	26	95.2±3.7	77.9±1.9	4.2	50	<0.001

Echo intensity values (resolution, 8 bits; black, 0; white, 255) were determined by gray-scale analysis of the echo signals detected during sonographic examination. Results of Student's t-test between transverse and longitudinal muscle echo intensity signals for each plane are also given. See Results for details.

DISCUSSION

Here, we applied a non-invasive method to identify and distinguish internal parts of the arm of *O. vulgaris*. Ultrasonographic scanning on the three anatomical planes allowed the identification of different structures as they appear in the classic morphological study.

The dimensions of the arm and its structures, obtained by an ultrasonographic approach and post mortem appeared to be significantly correlated. This provides the possibility of evaluating differences between arms of the same and/or different individuals. In addition, we also determined muscle echo intensity, finding different reflectivity on the basis of the arrangement of fibers and their intimate relationship with other tissues. As in other studies, our data confirmed the strong correlation between muscle structure and muscle echo intensity (Scholten et al., 2003; Pillen et al., 2009).

Our approach is based on a common practice in ultrasound examination in higher vertebrates and it allows, for the first time, quantitative analysis of images in an invertebrate. However, it is crucial that all system parameters and settings are constant in every measurement. In our conditions, for each arm we used the exact same site of measurement, at an anatomically defined location, in order to ensure that different individuals could be compared. We also standardized the timing of ultrasound examination by keeping animals in the anesthetic solution for the same length of time; this allowed the examination of arms in the same relaxed conditions.

Similar to other studies (e.g. Pillen et al., 2009), measurements obtained in our study of an octopus arm are very weakly influenced by changes in probe position because of the constancy and standardization of the sonographic examination. Therefore, we suggest that the variance in echo intensity we observed corresponds to differences in the structures within the octopus arm (e.g. connective tissue in the lateral longitudinal fibers).

In order to potentially measure changes in muscle thickness and/or echo intensity due to, for example, active contraction of the arm, it will be crucial to reach the exact scanning plane with reference to the anatomical position.

Ultrasonography has already been applied on cephalopods to examine internal structures, like inside the mantle (Davenport, 1993; King et al., 2005; King and Adamo, 2006) or the brain (Grimaldi et al., 2007). Ultrasound is thus confirmed to be a powerful tool that allows investigation of the behavior, physiology and biomechanics of the arm in the living animal, by a non-invasive method. In this way it is possible to understand the real characteristics of a structure, preserving its properties and observing it under natural conditions.

ACKNOWLEDGEMENTS

The authors are grateful to Anna Maria Grimaldi and the staff of the G.F. Lab at the Stazione Zoologica for assistance. We also thank anonymous reviewers for their helpful suggestions on an earlier draft of the manuscript.

FUNDING

This work was supported by Scuola Superiore Sant'Anna [grant no.??? to G.P.] and by Istituto Banco di Napoli, Fondazione [grant no.??? to G.P. and G.F.].

REFERENCES

Abramoff, M. D., Magelhaes, P. J. and Ram, S. J. (2004). Image processing with ImageJ. *Biophotonics Int.* **11**, 36-42.

Borrelli, L., Gherardi, F. and Fiorito, G. (2006). *A Catalogue of Body Patterning in Cephalopoda*, 614 pp. Firenze: Firenze University Press.

Chichery, M. P. and Chichery, R. (1988). Manipulative motor activity of the cuttlefish *Sepia officinalis* during prey capture. *Behav. Processes* **17**, 45-56.

Colasanti, G. (1876). Anatomische und Physiologische Untersuchungen über den Arm der Kephalopoden. *Arch. Anat. Physiol. Wissenchaftliche Med.* **9**, 480-500.

Cuvier, G. (1817). *Mémoires Pour Servir à L'histoire et à L'anatomie des Mollusques. Mémoires sur les Céphalopodes et sur leur Anatomie.* pp. 1-54. Paris: Deterville.

Davenport, J. (1993). Ultrasonography-a noninvasive tool for the study of structure and mechanical events in marine animals. *J. Mar. Biol. Assoc. UK* **73**, 461-464.

Dilly, N., Nixon, M. and Packard, A. (1964). Forces exerted by *Octopus vulgaris*. *Pubbl. Staz. Zool. Napoli* **34**, 86-97.

Finn, J. K., Tregenza, T. and Norman, M. D. (2009). Defensive tool use in a coconut-carrying octopus. *Curr. Biol.* **19**, R1069-R1070.

Fiorito, G., Von Planta, C. and Scotto, P. (1990). Problem-solving ability of *Octopus vulgaris* Lamarck (Mollusca, Cephalopoda). *Behav. Neural Biol.* **53**, 217-230.

Goldstein, R. B., Filly, R. A. and Simpson, G. (1987). Pitfalls in femur length measurements. *J. Ultrasound Med.* **6**, 203-207.

Grasso, F. W. (2008). Octopus sucker-arm coordination in grasping and manipulation. *Am. Malacol. Bull.* **24**, 13-23.

Graziadei, P. (1971). The nervous system of the arms. In *The Anatomy of the Nervous System of Octopus vulgaris* (ed. J. Z. Young), pp. 45-61. Oxford: Clarendon Press.

Grimaldi, A. M., Agnisola, C. and Fiorito, G. (2007). Using ultrasound to estimate brain size in the cephalopod *Octopus vulgaris* Cuvier *in vivo*. *Brain Res.* **1183**, 66-73.

Guérin, J. (1908). Contribution à l'étude des systèmes cutané, musculaire et nerveux de l'appareil tentaculaire des céphalopodes. *Arch. Zool. Exp. Gen.* **38**, 1-178.

Gutfreund, Y., Flash, T., Yarom, Y., Fiorito, G., Segev, I. and Hochner, B. (1996). Organization of octopus arm movements: a model system for studying the control of flexible arms. *J. Neurosci.* **16**, 7297-7307.

Hanlon, R. T. and Messenger, J. B. (1996). *Cephalopod Behaviour*. Cambridge, UK: Cambridge University Press.

House, M. R. (1988). Major features of cephalopod evolution. In *Cephalopods, Present and Past* (ed. J. Wiedmann and J. Kullmann), pp. 1-16. Stuttgart: Schweizerbart.

Huffard, C. L., Boneka, F. and Full, R. J. (2005). Underwater bipedal locomotion by octopuses in disguise. *Science* **307**, 1927.

Kier, W. M. (1982). The functional-morphology of the musculature of squid (Loliginidae) arms and tentacles. *J. Morphol.* **172**, 179-192.

Kier, W. M. (1985). The musculature of squid arms and tentacles-ultrastructural evidence for functional differences. *J. Morphol.* **185**, 223-239.

Kier, W. M. (1992). Hydrostatic skeletons and muscular hydrostats. In *Biomechanics (Structures and Systems): A Practical Approach* (ed. A. A. Biewener), pp. 205-231. Oxford, UK: IRL Press.

Kier, W. M. and Smith, K. K. (1985). Tongues, tentacles and trunks-the biomechanics of movement in muscular-hydrostats. *Zool. J. Linn. Soc.* **83**, 307-324.

Kier, W. M. and Stella, M. P. (2007). The arrangement and function of octopus arm musculature and connective tissue. *J. Morphol.* **268**, 831-843.

King, A. J. and Adamo, S. A. (2006). The ventilatory, cardiac and behavioural responses of resting cuttlefish (*Sepia officinalis* L.) to sudden visual stimuli. *J. Exp. Biol.* **209**, 1101-1111.

King, A. J., Henderson, S. M., Schmidt, M. H., Cole, A. G. and Adamo, S. A. (2005). Using ultrasound to understand vascular and mantle contributions to venous return in the cephalopod *Sepia officinalis* L. *J. Exp. Biol.* **208**, 2071-2082.

Laschi, C., Mazzolai, B., Mattoli, V., Cianchetti, M. and Dario, P. (2009). Design of a biomimetic robotic octopus arm. *Bioinspir. Biomim.* **4**, 015006.

Mather, J. A. (1998). How do octopuses use their arms? *J. Comp. Psychol.* **112**, 306-316.

Messenger, J. B., Nixon, M. and Ryan, K. P. (1985). Magnesium chloride as an anesthetic for Cephalopods. *Comp. Biochem. Physiol.* **82C**, 203-205.

Packard, A. (1972). Cephalopods and fish: the limits of convergence. *Biol. Rev.* **47**, 241-307.

Pillen, S., van Dijk, J. P., Weijers, G., Raijmann, W., de Korte, C. L. and Zwarts, M. J. (2009). Quantitative gray-scale analysis in skeletal muscle ultrasound: a comparison study of two ultrasound devices. *Muscle Nerve* **39**, 781-786.

Runnegar, B. and Pojeta, J. (1974). Molluscan phylogeny-paleontological viewpoint. *Science* **186**, 311-317.

Scholten, R. R., Pillen, S., Verrips, A. and Zwarts, M. J. (2003). Quantitative ultrasonography of skeletal muscles in children: normal values. *Muscle Nerve* **27**, 693-698.

Sumbre, G., Gutfreund, Y., Fiorito, G., Flash, T. and Hochner, B. (2001). Control of octopus arm extension by a peripheral motor program. *Science* **293**, 1845-1848.

Sumbre, G., Fiorito, G., Flash, T. and Hochner, B. (2005). Motor control of flexible octopus arms. *Nature* **433**, 595-596.

Walker, I. D., Dawson, D., Flash, T., Grasso, F., Hanlon, R., Hochner, B., Kier, W. M., Pagano, C., Rahn, C. D. and Zhang, Q. (2005). Continuum robot arms inspired by cephalopods. Proceedings SPIE Conference on Unmanned Ground Vehicle Technology VII. Orlando, FL, pp. 303-314.

Wells, M. J. (1978). *Octopus. Physiology and Behaviour of an Advanced Invertebrate*, 420pp. London: Chapman and Hall.

Zagzebski, J. A. (1996). *Essentials of Ultrasound Physics*, 220pp. St Louis, Missouri: Mosby, Inc.